



Inorganic Carbon Leaching From a Warmed and Irrigated Carbonate Forest Soil

Andreas Schindlbacher^{1*}, Kerstin Beck², Stefan Holzheu³ and Werner Borcken^{2*}

¹ Department of Forest Ecology, Federal Research and Training Centre for Forests, Natural Hazards and Landscape-BFW, Vienna, Austria, ² Department of Soil Ecology, University of Bayreuth, Bayreuth, Germany, ³ BayCEER, University of Bayreuth, Bayreuth, Germany

OPEN ACCESS

Edited by:

Douglas Godbold,
University of Natural Resources and
Life Sciences Vienna, Austria

Reviewed by:

Corey R. Lawrence,
United States Geological Survey
(USGS), United States
Zachary E. Kayler,
University of Idaho, United States

*Correspondence:

Andreas Schindlbacher
andreas.schindlbacher@bfw.gv.at
Werner Borcken
werner.borcken@uni-bayreuth.de

Specialty section:

This article was submitted to
Forest Soils,
a section of the journal
Frontiers in Forests and Global
Change

Received: 19 February 2019

Accepted: 08 July 2019

Published: 02 August 2019

Citation:

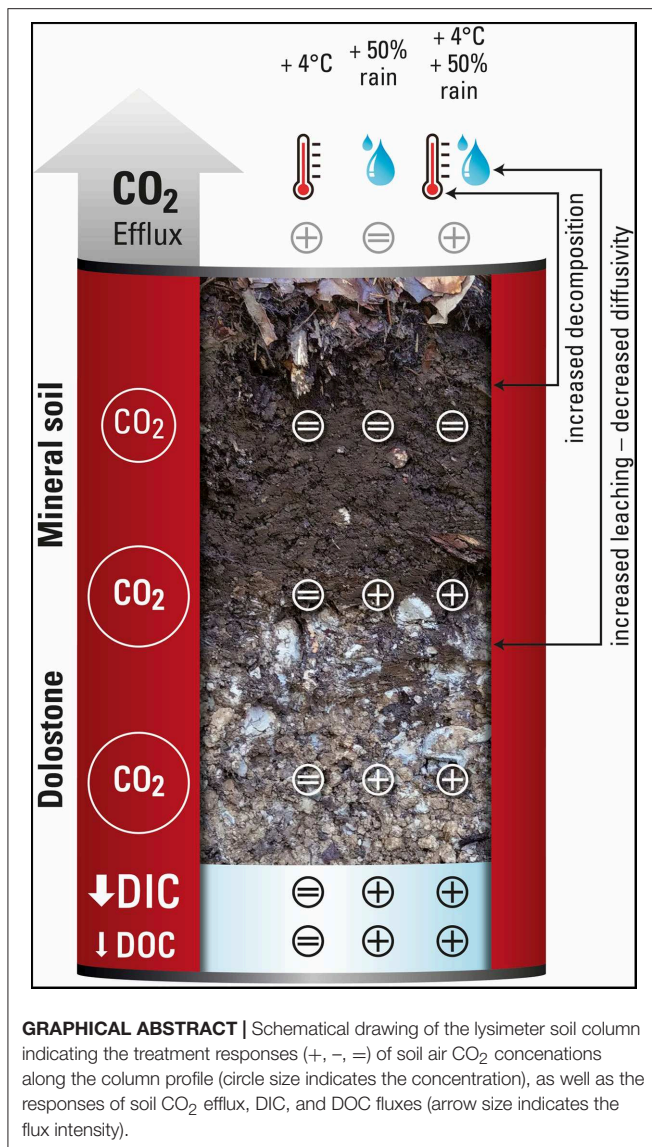
Schindlbacher A, Beck K, Holzheu S
and Borcken W (2019) Inorganic
Carbon Leaching From a Warmed and
Irrigated Carbonate Forest Soil.
Front. For. Glob. Change 2:40.
doi: 10.3389/ffgc.2019.00040

The response of dissolved inorganic carbon (DIC) leaching to rising temperature and precipitation is hardly known for forest soils on carbonate bedrock. We established field lysimeters, filled with soil from a humus-rich A horizon of a Rendzic Leptosol and detrital dolomite (C horizon) and conducted a two-factorial climate manipulation [control (C), soil warming (H, +4°C), irrigation (I, +50% precipitation), soil warming and irrigation (H+I)] to examine the effects of increased temperature and precipitation on DIC and DOC leaching, soil air CO₂ concentrations, and soil CO₂ efflux. We followed an isotopic approach to assess the biotic and abiotic DIC fractions. Soil warming (H) had no effect on DIC leaching and seepage DIC concentrations. Irrigation (I and H+I) increased annual DIC leaching by almost 100% as a matter of significantly increased seepage DIC concentrations and higher annual drainage. Isotopic partitioning of DIC fluxes suggested biotic contributions between 60 and 100% and no significant variation with warming or irrigation. Soil warming consistently increased the soil CO₂ efflux by >50% independently of irrigation treatment. Soil air CO₂ concentrations were not affected by soil warming alone (H). Irrigation (I and I+H) tended to increase subsoil (18 and 32 cm depth) soil air CO₂ concentrations, while topsoil (6 cm) remained unaffected by irrigation. DIC leaching losses were about 4–5 times higher than DOC leaching losses, which showed a similar treatment response (I and H+I > C and H). Annual DIC leaching amounted to between 20 ± 2 (C) and 39 ± 2 (H+I) g m⁻², representing ~ 2–5% of the total annual gaseous soil CO₂ loss. Our results suggest that climate change, especially changing precipitation, could significantly affect the DIC export from carbonate forest soils, thereby affecting their carbon sequestration potential.

Keywords: DIC, carbonate soil, soil CO₂ efflux, DOC, δ¹³C, soil warming, irrigation, leaching

INTRODUCTION

Leaching of dissolved inorganic carbon (DIC) can affect the net ecosystem carbon balance and the soil organic carbon (SOC) budget of forest ecosystems (Kindler et al., 2011; Siemens et al., 2012). Soil solution DIC concentrations are generally higher in carbonate soils than in silicate soils (Jin et al., 2009; Kindler et al., 2011). If drainage predominates over transpiration, leaching of DIC can cause significant C losses from carbonate soils (Amiotte-Suchet et al., 1999; Ogrinc et al., 2016).



Mountain forests along the Northern Limestone Alps in Europe feature all the prerequisites for DIC leaching. The Northern Limestone Alps act as weather barrier from the north, triggering cloud formation, and regional precipitation (up to 2,500 mm y⁻¹) (Frei and Schär, 1998). Soils along the mountain range are formed on dolomite or limestone bedrock and can contain high amounts of carbonate, even in the topsoil (Kloss et al., 2012; Christophel et al., 2015; Schindlbacher et al., 2015a). Climate change likely affects DIC leaching from these soils, since temperature, precipitation, and CO₂ partial pressure have great impact on the formation and flux of DIC. A recent study reports a strong decline in SOC stocks in the German part of the Northern Limestone Alps during the past decades and attributes it to ongoing climate warming (Prietz et al., 2016). A long-term artificial soil warming experiment in the neighboring Austrian Alps suggest enhanced decomposition of soil organic matter (SOM) due to warming (Schindlbacher et al., 2015b). The potential role of

DIC leaching under changing climatic conditions is, however, yet unknown.

DIC consists of four components: dissolved CO₂, carbonic acid (H₂CO₃), bicarbonate (HCO₃⁻), and carbonate (CO₃²⁻). Both, the distribution as well as the concentration of these components in soil water is strongly pH-dependent. Carbonate weathering stabilizes the soil pH around neutral and serves as a temporal sink of CO₂ from the soil atmosphere, following CO₂ dissolution, and the formation and dissociation of H₂CO₃:



where MCO₃ is for example calcite (CaCO₃) or dolomite (CaMg(CO₃)₂). The carbonate weathering rate and the CO₂ fixation/release rates rely on many factors such as the physical and chemical properties of carbonate, soil CO₂ concentrations, temperature, water content, and water flow, i.e., removal of HCO₃⁻ to groundwater (e.g., Szramek et al., 2007; Clark, 2015). At equilibrium (Equation 1), approximately one half of the exported HCO₃⁻ derives from biotic sources (CO₂ from respired SOC and root respiration) and the other half from the abiotic source (carbonate bedrock). Partitioning of biotic and abiotic DIC in seepage can be achieved by isotopic mass balance and allows estimating the potential leaching loss of inorganic carbon from the soil (Karberg et al., 2005; Kindler et al., 2011).

Aside DIC leaching, leaching of dissolved organic carbon (DOC) represents another loss of biotic carbon from soils. DOC losses from soils can strongly vary among forest sites as many factors control the production and fate of DOC (Camino-Serrano et al., 2014). Thin forest floors as main DOC source mostly lead to small DOC leaching from calcareous forest soils, however, DOC fluxes also rely on the local precipitation and temperature regime (Borken et al., 2011). How rising temperature and changing precipitation will affect DOC leaching from these calcareous forest soils is yet not clear either.

Rising temperature and changing precipitation affect the decomposition of SOM and thus the soil CO₂ efflux (e.g., Orchard and Cook, 1983; Fang and Moncrieff, 2001; Borken and Matzner, 2009) which is physically controlled by the vertical gradient of soil CO₂ concentration and the CO₂ transport within the soil (Davidson et al., 2006). CO₂ concentration typically increases with soil depth up to a maximum, coincided with ¹³C enrichment of CO₂ due to kinetic fractionation (Amundson et al., 1998). Climatic change could thus not only alter soil CO₂ concentrations, but also DIC concentration of seepage and DIC leaching from calcareous soils.

In the current study we simulated a potential climate change scenario and assessed effects on DIC leaching, DOC leaching, and soil CO₂ efflux from a model soil. Calcareous soils, such as in the Northern Limestone Alps are characterized by pronounced spatial heterogeneity in soil depth, carbonate content, and total organic carbon stock (Prietz et al., 2014). Such heterogeneities lead to high spatial variability in soil CO₂ concentration, soil CO₂ efflux (Schindlbacher et al., 2012) and DOC, as well as DIC (Kindler et al., 2011). Accordingly, the design of *in-situ* field experiments to study organic (soil

carbon) and inorganic (carbonate weathering) interactions in combination with complex climatic manipulations would require high replication and would be extremely costly. We therefore choose a controlled experimental setting with uniformly packed soil columns and defined climate treatments. For this purpose, columns were packed with calcareous forest soil and dolomite detritus originating from the long-term climate manipulation site Achenkirch, Austria (Schindlbacher et al., 2012). Columns then acted as field lysimeters and a two-factorial (soil warming, irrigation) climate-manipulation was initiated. We chose a +4°C warming treatment to simulate potential soil temperatures within the end of the century (IPCC, 2013) and to allow for comparability with previous results from the Achenkirch climate manipulation experiment (Schindlbacher et al., 2009). In addition to rising temperatures, an overall increase in annual precipitation in the Northern limestone Alps is predicted by regional climate models (e.g., Smiatek et al., 2016). We therefore artificially increased natural precipitation by ~50%.

We hypothesized that (H1) soil warming alone would increase SOM decomposition, thereby increasing soil air CO₂ concentrations and soil surface efflux. Higher soil air CO₂ concentrations would increase DIC concentrations, resulting in increased DIC leaching; (H2) increased rainfall alone would not affect SOM decomposition, but would increase DIC leaching as a matter of increased drainage. Finally, we hypothesized that (H3) a combination of warming and increased rainfall would lead to highest DIC leaching losses due to increased DIC concentrations (warming), combined with higher drainage (increased rainfall). Leaching losses of DOC were expected to be of minor importance, since most of the DOC was assumed to be consumed and respired by decomposer microorganisms.

MATERIALS AND METHODS

Experimental Setup

The experiment was set up with a total of 20 lysimeters at a meadow in Bayreuth (49°57'37.5"N, 11°35'45.7"E), Germany, in autumn 2015. Mineral soil (A horizon) and fresh leaf litter of European beech were taken in August and October 2015 from a forest site located in the Northern Limestone Alps at about 910 m a.s.l. near Achenkirch, Austria (47°34'50"N, 11°38'21"E). The 10–40 cm thick soil, a Rendzic Leptosol (FAO, 1998) with A-A/C-C horizons developed on dolomite bedrock. The A horizon had a loamy-clay texture and was characterized by a high organic carbon content of 14%, a C/N ratio of 18, a carbonate content of about 5% and a pH (CaCl₂) of ~7. Mean bulk density of the A horizon (0–10 cm depth) was ~0.55 g cm⁻³ (Schindlbacher et al., 2010). Further details of the site and soil properties are given in Schindlbacher et al. (2015b). Detrital dolomite of glacial dolomite with a carbonate content of >99% was sampled close to the forest site. For the experiment, mineral soil was sieved (1 cm), and live plant material was sorted out. Detrital dolomite gravel with diameters of 1–8 cm was washed with tap water to remove soil particles and organic debris.

A lysimeter consisted of a cylindrical high-density polyethylene (HDPE) bucket (Paul Craemer GmbH, Herzebrock-Clarholz, Germany) with a height of 51 cm and an inner diameter

of 45.5 cm (Figure S1). At the bottom a polycarbonate drainage panel with a height of 5 cm was placed for seepage sampling. Detrital dolomite was filled between 46 and 21 cm depth with a bulk density of 1.5 g cm⁻³ (60.7 kg d.w.), followed by mineral soil from 21 to 1 cm depth with a bulk density of 0.5 g cm⁻³ (15.1 kg d.w.). A gauze with a mesh size of 290 μm was inserted on the drainage panel and between dolomite and mineral soil to prevent particle movement. A litter layer was simulated by adding 400 g d.w. m⁻² beech litter on top of the mineral soil.

In half of the lysimeters, heating cables (length 2.5 m, 230 V, 37.5 W, A. Rak Wärmetechnik GmbH, Frankfurt, Germany) were buried in a spiral pattern at 8 and at 20 cm depth from the mineral soil surface in order to allow for homogenous soil warming (Figure S1). All lysimeters were equipped with temperature sensors (Dallas One Wire, waterproof DS18B20) at 0, 8, 20, and 32 cm depth.

A soil moisture probe (EC10, Decagon, Pullman, USA) was placed to record hourly volumetric water contents at 7.5 cm soil depth (Figure S1). A soil-specific calibration of the moisture probes (MP) was conducted to convert the readings into volumetric water contents (VWC): $VWC = 1.07MP - 0.50$ ($R^2 = 0.98$), where VWC is in cm³ cm⁻³ and MP in mV. For the calibration, a cylinder (15 cm diameter, 20 cm height) was filled with air-dried soil, equipped with a moisture probe, and then compacted to a bulk density of 0.5 g cm⁻³. Amounts of 100–200 ml water were stepwise added to the soil up to water saturation within 8 weeks. Readings of the moisture probe and the soil weight were recorded before and after each water addition. Afterwards, the water-saturated soil was drained and then dried at 105°C for determination of field capacity and total pore volume.

Perforated polycarbonate tubes (length 10 cm, diameter 1.6 cm, pore diameter 3 mm) attached to stainless steel capillary tubes (3 mm outer diameter) were installed centrally at 6, 18, and 32 cm soil depth for soil gas sampling. On the edge of the lysimeter, a polyethylene (PE) tube (length 1 m, outer diameter 4 mm) was laid which reached from the bottom of the water reservoir outwards. In addition, a PVC collar (height 11 cm, diameter 15 cm) was inserted 3 cm into the soil to measure soil CO₂ efflux based on the dynamic closed chamber method.

The 20 lysimeters were buried into the soil at ground level in five rows with a distance of 2 m between the rows and a distance of 1.2 m between the lysimeters within the rows in October/November 2015. Each of the five rows consisted of four treatments: control (C), heating (H), irrigation (I), and the combination of heating and irrigation (H+I) with a replication of 5 lysimeters ($n = 5$), each. The soil temperature in the warmed lysimeters was permanently increased by 4°C in comparison to the corresponding controls. The central unit of the temperature regulation was a raspberry pi model B+ (Figure S1). One raspberry pi controlled two units, one heated, and one control lysimeter. The temperature sensors were connected directly to the GPIO4 pin of the pi. To control the heating cables a power switch (solid state relay module, SainSmart, Lenexa, USA) was connected to the GPIO pins.

The irrigated lysimeters (H+I, I) received ~50% more annual precipitation. Rainwater was collected for irrigation at the field

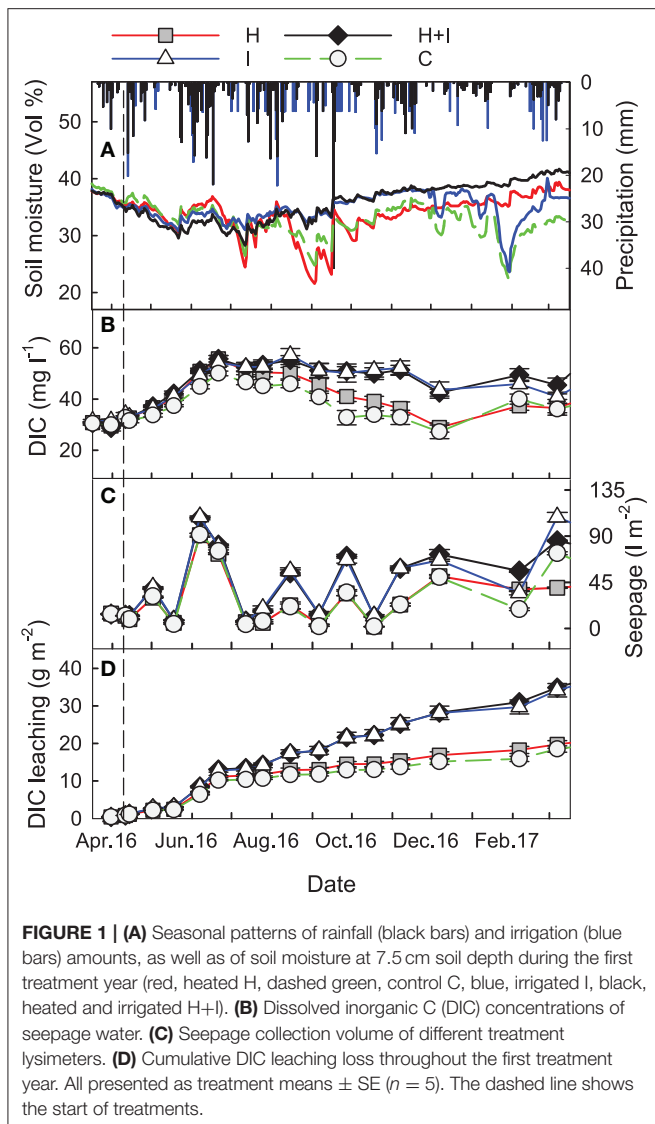


FIGURE 1 | (A) Seasonal patterns of rainfall (black bars) and irrigation (blue bars) amounts, as well as of soil moisture at 7.5 cm soil depth during the first treatment year (red, heated H, dashed green, control C, blue, irrigated I, black, heated and irrigated H+I). **(B)** Dissolved inorganic C (DIC) concentrations of seepage water. **(C)** Seepage collection volume of different treatment lysimeters. **(D)** Cumulative DIC leaching loss throughout the first treatment year. All presented as treatment means \pm SE ($n = 5$). The dashed line shows the start of treatments.

site using a 3 m² large PVC roof with PVC gutter and a rain barrel. This rainwater was applied to irrigated lysimeters at intervals from days to weeks, depending on the amount and pattern of rainfall (Figure 1). Maximum amounts of 1 L rainwater (equal to 6.15 mm) were irrigated per day and lysimeter using a watering can equipped with a sprinkler. No irrigation was performed 3 days before gas and water sampling. The amount of rainwater was measured with rain gauges (RS200, UP GmbH, Ibbenbüren, Germany) that were installed in 1 m height close to the lysimeters.

Soil Air CO₂ Concentrations and Seepage DIC Concentrations

Soil air CO₂ concentrations and DIC concentrations were measured every 2–3 weeks between March and November 2016. During winter 2016/17 and during 2017 sampling intervals were extended to 3–5 weeks. DIC measurements were completed in

April 2017 and soil air CO₂ measurements were completed in September 2017. Three measurements took place prior to the climate manipulations.

Glass vials (22 ml, IVA-Analysentechnik GmbH & Co. KG, Meerbusch, Germany) were sealed with butyl rubber septa and aluminum caps and flushed with pure nitrogen (N₂). For seepage sampling, 50 μ l of phosphoric acid (85%) was added to each vial before sealing to convert DIC into gaseous CO₂ in the vial headspace. Gas samples were taken at 6, 18, and 32 cm lysimeter depth (Figure S1). A 20 ml syringe was connected to a three-way stopcock with Luer lock, which was attached to the capillary tube. The first 11 ml gas sample was discarded to rinse the capillary tube and syringe. Then, another 11 ml gas sample was taken and injected into the vial. The mixing ratio of a gas sample in a vial (X_{sample}) was calculated after measuring the vial pressure (hPa) with a tensiometer pressure device and the atmospheric pressure (hPa) with a barometer as follows:

$$X_{\text{sample}} = \frac{\text{vial pressure} - \text{atmospheric pressure}}{\text{vial pressure}} \quad (2)$$

DIC sampling was done in a similar way, except that the first 20 ml seepage were discarded because of the greater tube volume. About 5 ml seepage sample was injected into the acid prepared vial without contact to the atmosphere. The exact sample volume was determined by weighing the vials after analysis.

The gaseous CO₂ concentrations in the vials were analyzed using a gas chromatograph (GC, 8610C, SRI Instruments, Torrance, USA) equipped with a silica gel column (length 1 m, diameter 3 mm, column temperature 130°C) and a flame ionization detector coupled to a methanizer (detector temperature 380°C). A sample volume of 100 μ l was injected directly onto the column. The measured CO₂ concentration in a vial ($\text{vial}_{\text{CO}_2}$) was back calculated to soil CO₂ concentration ($\text{soil}_{\text{CO}_2}$) according to its mixing ratio (X_{sample}) in that vial (Equation 2) as follows:

$$\text{soil}_{\text{CO}_2} = \frac{\text{vial}_{\text{CO}_2}}{X_{\text{sample}}} \quad (3)$$

The CO₂ concentration in the headspace of the vials containing seepage was determined by GC (see above) after shaking solutions at 150 rpm for 2 h and temperature adjustment to 20°C. The amount of headspace CO₂ (gas_{CO_2}) was used to calculate the amount of CO₂ in the aqueous phase (aq_{CO_2}) after Henry's law:

$$\text{aq}_{\text{CO}_2} = K_H \times \text{gas}_{\text{CO}_2} \times \frac{V_{\text{aq}}}{V_{\text{gas}}} \quad (4)$$

where K_H is the dimensionless Henry solubility constant of 0.90 for CO₂ in water at 293.15 K (Sander, 2015), aq_{CO_2} and gas_{CO_2} are expressed in (mol), V_{aq} and V_{gas} are the volumes (L) of the aqueous and gas phase in a vial, respectively. The DIC concentration in seepage results from the sum of aq_{CO_2} and gas_{CO_2} related to the seepage volume (L) in a vial.

Isotope Analysis

Isotope ratios of soil air CO₂ and seepage DIC were determined monthly from April 2016 until November 2016. Gas and seepage samples for stable isotope analysis were taken with 12 ml glass vials (Exetainer, Labco Ltd., Lampeter, UK) immediately after sampling for determination of CO₂ or DIC concentrations. Vial preparation and sampling were done in a similar way as described above.

The $\delta^{13}\text{C}$ values of CO₂ were determined using a coupled GC-Isotope ratio mass spectrometer (GC-IRMS, 5890 Series II, Hewlett-Packard, Wilmington, USA, Delta V Plus, Thermo Fisher Scientific, Bremen, Germany). The CO₂ working standard (3,000 ppmv) was calibrated against four IAEA standards (CO-1, CO-8, ANU sucrose, and NBS 18). Isotopic signatures were expressed in the common δ -notation as deviation in ‰ from the VPDB-standard according to Equation (5) where R is the ratio of heavy to light isotopes in the sample and the standard.

$$\delta = \left[\frac{R_{\text{sample}}}{R_{\text{standard}}} - 1 \right] \times 1000 \quad (5)$$

The precision of the $\delta^{13}\text{C}$ values was 0.2‰. The $\delta^{13}\text{C}$ value of DIC was calculated from the headspace $\delta^{13}\text{C}_{\text{CO}_2}$ value and corrected for isotopic fractionation between aqueous and gaseous phase in the vial by using Henry's law and a fractionation factor of 1.1‰ between CO_{2(g)} and CO_{2(aq)} (Vogel et al., 1970). The isotopic composition of CO₂ from microbial decay of SOM ($-28.5 \pm 0.4\text{‰}$, $n = 8$) was determined following incubation of mineral soil at 20°C in a vial flushed with synthetic air. The isotopic signatures of dolomite and bulk soil (A horizon) were $+3.1 \pm 0.1\text{‰}$ and $-23.6 \pm 0.3\text{‰}$, respectively, determined with an elemental-analyzer coupled to an IRMS (NA 1108, CE Instruments, Milan, Italy, Delta plus, ConFlo III interface, Thermo Fisher Scientific, Bremen, Germany).

Seepage Flux

Seepage in the drainage panel reservoir of each lysimeter was manually collected using a water pump and 10 L bottles. Total seepage amounts were measured by weighing filled bottles. Sampling of seepage took place after gas sampling and if necessary after heavy rainfall events between gas sampling dates. The cumulative seepage flux (mm) between gas sampling dates was calculated by multiplying the amount of collected seepage with the soil surface area.

DIC Leaching and Carbon Source Partitioning

An isotope mass balance approach was applied to assess the contribution of carbonate weathering (abiotic) and of soil air CO₂ (respired, biotic) to the total DIC flux using the following Equations:

$$\delta^{13}\text{C}_{\text{DIC}} \times F_{\text{DIC}} = \delta^{13}\text{C}_{\text{Soil CO}_2} \times F_{\text{DIC biotic}} + \delta^{13}\text{C}_{\text{Carbonate}} \times F_{\text{DIC abiotic}} \quad (6)$$

$$F_{\text{DIC}} = F_{\text{DIC biotic}} + F_{\text{DIC abiotic}} \quad (7)$$

where $\delta^{13}\text{C}_{\text{DIC}}$, $\delta^{13}\text{C}_{\text{Soil CO}_2}$, and $\delta^{13}\text{C}_{\text{Carbonate}}$ are the respective isotopic signatures and F_{DIC} , $F_{\text{DIC biotic}}$, and $F_{\text{DIC abiotic}}$ are fluxes. The DIC flux (F_{DIC}) was calculated by multiplying the DIC concentration with the cumulative seepage flux. We assume that the parameter $\delta^{13}\text{C}_{\text{Soil CO}_2}$ is best represented by the 18 cm depth in the transition from the A to C horizon. The $\delta^{13}\text{C}_{\text{Soil CO}_2}$ at 18 cm depth was corrected by 8–10‰ for temperature-dependent isotopic fractionation during dissolution of CO₂ and formation of HCO₃⁻ in water according to Zhang et al. (1995):

$$\varepsilon^{13}\text{C}(\text{CO}_{2(\text{g})} - \text{HCO}_3^-) = (-0.114 \times T) + 10.78 \quad (8)$$

where $\varepsilon^{13}\text{C}$ is the fractionation value and T is the temperature in °C at 20 cm depth. Considering the isotopic fractionation (Equation 8), the proportion of biotic and abiotic DIC was calculated by rearranging and inserting Equation (7) into Equation (6).

A second approach was used to assess the biotic fraction of DIC according to Kindler et al. (2011). The $\delta^{13}\text{C}$ of CO₂ from microbial respiration ($-28.5 \pm 0.4\text{‰}$) underlies fractionation processes by diffusive and advective transport along the CO₂ gradient from the lysimeter bottom to the atmosphere. This isotopic fractionation of CO₂ can vary with season and among soils (Jin et al., 2009). To account for the uncertainty caused by the enrichment of ¹³C in soil air CO₂, we substituted $\delta^{13}\text{C}_{\text{Soil CO}_2}$ in Equation 6 by a constant value for microbial respiration (-28.5‰) after correction for temperature-dependent fractionation (Equation 8). The applied isotope mass balance approach assumes that the abiotic DIC fraction results only from dolomite weathering by carbonic acid.

The Keeling plot approach (Keeling, 1961) was applied to determine the isotopic signature of the source of CO₂ in the lysimeters by plotting the inverse of CO₂ concentration in soil against the corresponding ¹³C signature of CO₂. The intercept of the linear regression, corrected by 4.4‰ to account for isotopic fractionation due to diffusion of CO₂ in the soil atmosphere (Amundson et al., 1998), represents the CO₂ source.

DOC Leaching

DOC concentrations of seepage were analyzed of pooled samples from each lysimeter and rainfall collector at seven occasions between March 2016 and April 2017. Samples for DOC and DIC analysis were taken at the same time (see section Soil air CO₂ concentrations and seepage DIC concentrations), but samples for DOC analysis were immediately frozen at -24°C after sampling. For further processing, all samples of a 2-month interval as well as samples of the pretreatment period were pooled to one sample per lysimeter. Pooled samples were then filtered with 0.45 μm cellulose-acetate filter and analyzed using elemental analysis (multi N/C 2100 Analyzer, Analytik Jena, Germany). DOC fluxes were calculated by multiplying DOC concentration with the sum of rainwater or seepage of the respective sampling interval.

Soil CO₂ Efflux

Soil CO₂ efflux was measured with the closed dynamic chamber technique as described in detail by Savage and Davidson (2003).

Briefly, the PVC ring was manually sealed with a PVC lid for a measurement. Air circulated between the chamber (1.75 L volume) and an infrared gas analyzer (IRGA, LI-820, LICOR Biosciences GmbH, Lincoln, USA) with a rate of 0.5 L min⁻¹. A logger connected to the IRGA recorded the CO₂ concentration increase in the chamber headspace every 10 s for a period of 4 min. The soil CO₂ efflux was calculated from the linear increase of CO₂ concentration over time, and corrected for atmospheric pressure and air temperature in the headspace. Soil CO₂ efflux measurements took place between 10:00 a.m. and 12:00 a.m. using two IRGA systems to reduce the total measuring time. Individual lysimeters were measured in full random order to avoid any bias due to diurnal variations of the soil CO₂ efflux. Soil CO₂ efflux was measured approximately every 2–3 weeks between Mar 2016 and Jan 2018. Three measurements took place prior the start of the climate manipulations. The cumulative soil CO₂ efflux was estimated by linear interpolation between individual efflux measurement dates. Cumulative fluxes therefore represent rough estimates which do not account for diurnal efflux variations and temporal flux variations between the consecutive measurement dates. The cumulative estimates, however, were considered sufficiently robust for a comparison between lysimeter and field (Achenkirch, Northern Limestone Alps) fluxes.

Data Analysis

Depending on the availability of personal resources, measurements of target parameters (DIC, DOC, soil air CO₂, soil CO₂ efflux) were accomplished throughout different timeframes. During the first treatment year (Apr 2016–Apr 2017), all parameters were measured at the same 2–3 weekly resolution. Soil CO₂ efflux was measured for another full season (2017), whereas soil air CO₂ concentration measurements were completed in Sept 2017 and DIC, as well as DOC measurements were completed in April 2017 already. Treatment effects on individual target parameters were statistically tested over their full measurement duration. Cumulative carbon fluxes of the corresponding individual parameters were calculated for the first treatment year for further comparison.

Treatment effects on repeatedly measured soil air CO₂ concentrations, soil CO₂ efflux, seepage DIC, and DOC concentrations and ¹³C signatures of soil air CO₂ and seepage DIC were analyzed using linear mixed effect models (lme) as implemented in the R package nlme. Individual lysimeters of each treatment were added as a random factor into the model to account for the repeated measurement design. General linear hypotheses based on Tukey all-pair comparisons were conducted at a significance level of $P < 0.05$ for pair-wise *post-hoc* comparisons, using the R package multcompView. Significant differences of cumulative soil CO₂ effluxes, as well as of cumulative DIC and DOC leaching among the treatments (C, H, I, H+I), were tested using a one-way ANOVA. Analyses were performed using the R software (version 3.4.2).

RESULTS

Soil Warming and Precipitation Manipulation

Soil temperatures showed only small variations among the treatments ($cv = 3\%$ among the 20 lysimeters) during the pre-treatment period (**Figure S2**). Soil warming (H and H+I) had an immediate effect on soil temperature at all soil depths (**Figure S2**). Soil temperatures of the H and H+I treatments were consistently 4.0°C higher between 5 and 25 cm depth throughout the treatment period (**Figure 2C**; **Figure S2**). The warming effect slightly decreased by about 1–2°C toward the soil surface and bottom of the H and H+I lysimeters (**Figure S2**).

Rainfall amounted 537 mm from March to Dec 2016 and 787 mm from Jan 2017 to Jan 2018. Irrigation was performed from April 2016 to the end of December 2017 and resulted in a total additional precipitation input of 272 mm (+ 51%) during the first treatment year and 307 mm (+39%) during the second treatment year.

Pre-treatment soil moisture at 7.5 cm depth was around 40 vol% and all lysimeters showed similar soil moisture patterns during the first treatment months. In July 2016, a short dry period let soil moisture in C and H drop to around 25 vol%, whereas moisture in I and HI remained at higher levels (**Figure 1**). Similar patterns occurred during a longer dry period in late August to September 2016, during which soil moisture in C and H was about 10 vol% lower than in I and HI (**Figure 1**). During January 2017, soil freezing caused a further moisture-drop in unwarmed (I and HI) lysimeters, while warmed lysimeters remained unaffected from freezing. A more pronounced dry period from June to August 2017 let soil moisture in C and H decline into the range of 20 vol% while I and HI showed ~10% higher moisture contents (data not shown). The average pH of seepage from all lysimeters was 7.5 at six sampling occasions in 2017. Treatment and sampling date had no effect on pH in seepage.

DIC Leaching

Seepage DIC concentrations were significantly ($p < 0.001$) higher in the irrigated (H+I and I) lysimeters when compared to the C and H lysimeters. Differences in seepage DIC concentrations among treatments were small during the first three treatment months, but differences increased during the latter part of the year (treatment:date interaction $p < 0.001$) because of declining DIC concentration in the C and H lysimeters (**Figure 1B**). A similar pattern was observed for seepage flux (**Figure 1C**). In the pre-treatment period, all 20 lysimeters showed a mean seepage accumulation of 26.6 ± 1.0 mm with correspondingly low spatial variation ($cv = 4\%$). After 1 year treatment, seepage fluxes were 474 and 490 mm y⁻¹ at H and C lysimeters, and 765 and 770 mm y⁻¹ at H+I and I lysimeters, respectively. The evaporation loss (the difference between rainfall and seepage flux) did not differ significantly among treatments and ranged between 29 (H) and 21 (I)% of total rainfall input. Along with DIC concentrations and seepage fluxes, DIC leaching did not differ among the 20 lysimeters during the pre-treatment period (0.83 ± 0.05 g C m⁻²; $cv = 6\%$). Irrigation significantly ($p < 0.001$) increased annual

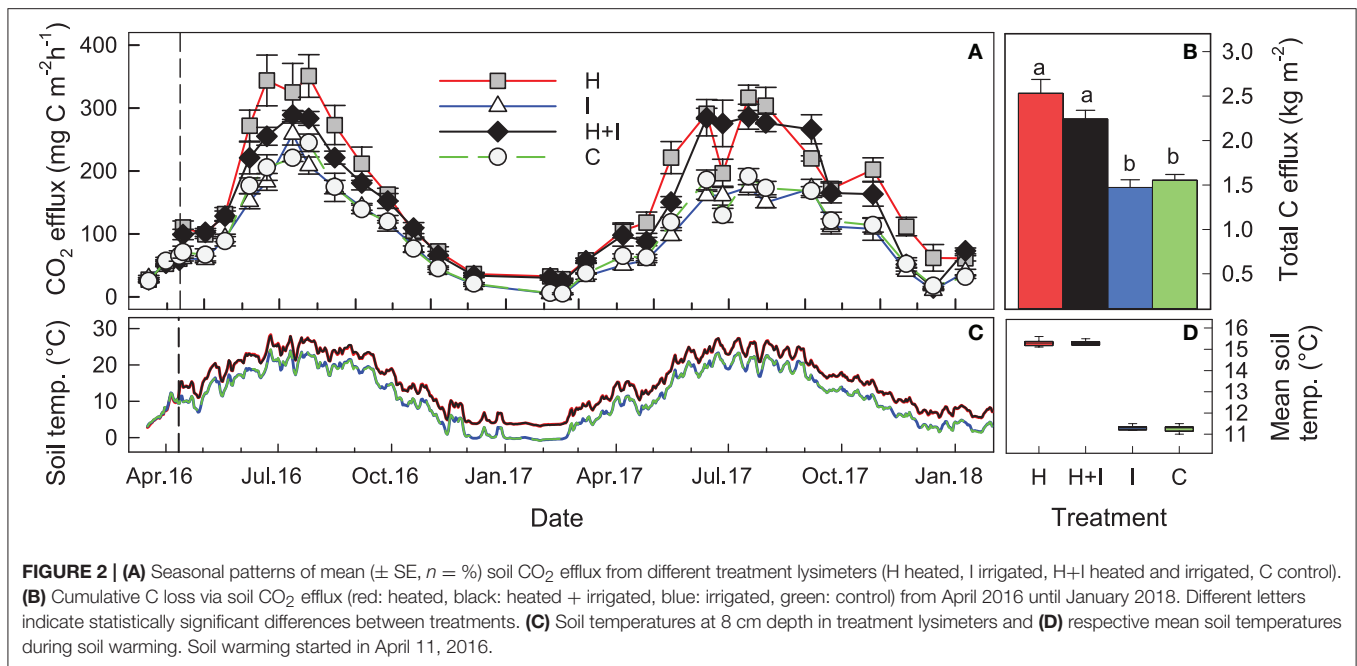


TABLE 1 | Annual soil carbon fluxes of four treatments (C control, I irrigated, H heated, H+I heated + irrigated) from April 2016 until April 2017.

| Treatment | $\text{CO}_2\text{-C}$ ($\text{g m}^{-2} \text{y}^{-1}$) | DIC ($\text{g m}^{-2} \text{y}^{-1}$) | DOC ($\text{g m}^{-2} \text{y}^{-1}$) |
|-----------|--|---|---|
| C | 795 (34) a | 20 (2) a | 4.8 (0.1) a |
| I | 765 (44) a | 37 (4) b | 6.9 (0.2) b |
| H | 1233 (103) b | 21 (2) a | 5.2 (0.1) a |
| H+I | 1073 (60) b | 39 (2) b | 7.7 (0.1) c |

Numbers are means and standard errors in brackets ($n = 5$). Different letters indicate statistically significant differences among treatments.

DIC leaching at I and H+I, almost doubling annual DIC leaching rates from C and H (Table 1).

Isotopic signatures of seepage DIC did not differ among the four treatments and ranged between -12.5 and -16.3% , fluctuating with seasons and showing most negative values during August and September (Figure 3). According to the isotopic mass balance (Equations 6, 7) and the measured isotopic signatures of seepage DIC, the contribution of biotic carbon to DIC ranged between 92 and $>100\%$ (Figure 4). When instead using a fixed end-member of -28.5% (the signature of microbial respiration) for biotic carbon, the biotic contribution to DIC leaching ranged between 68 and 90% (Figure 4).

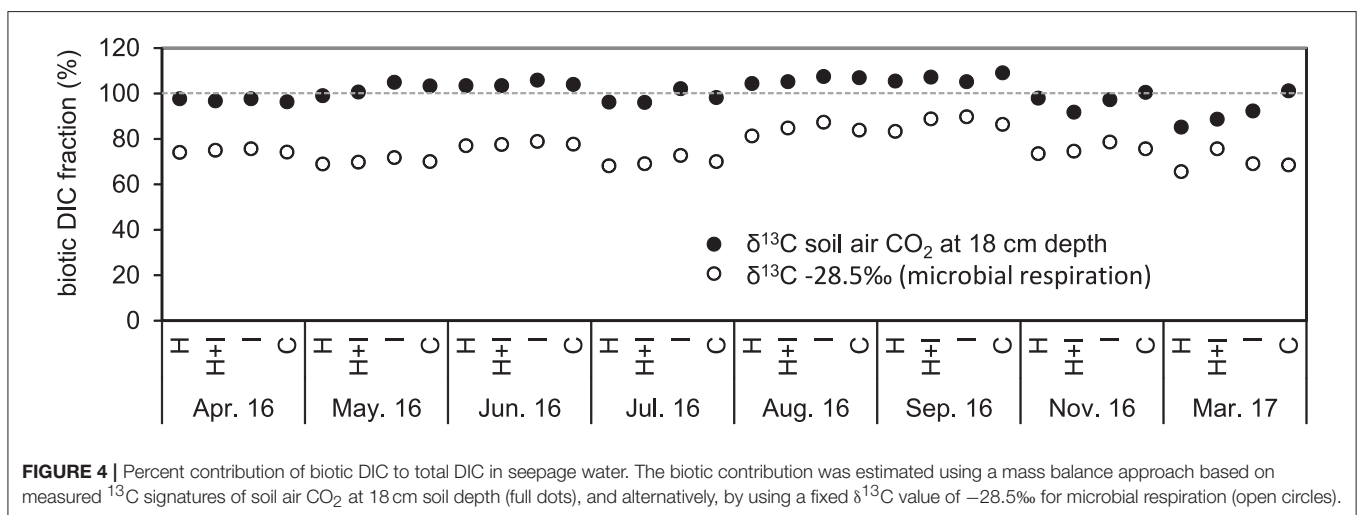
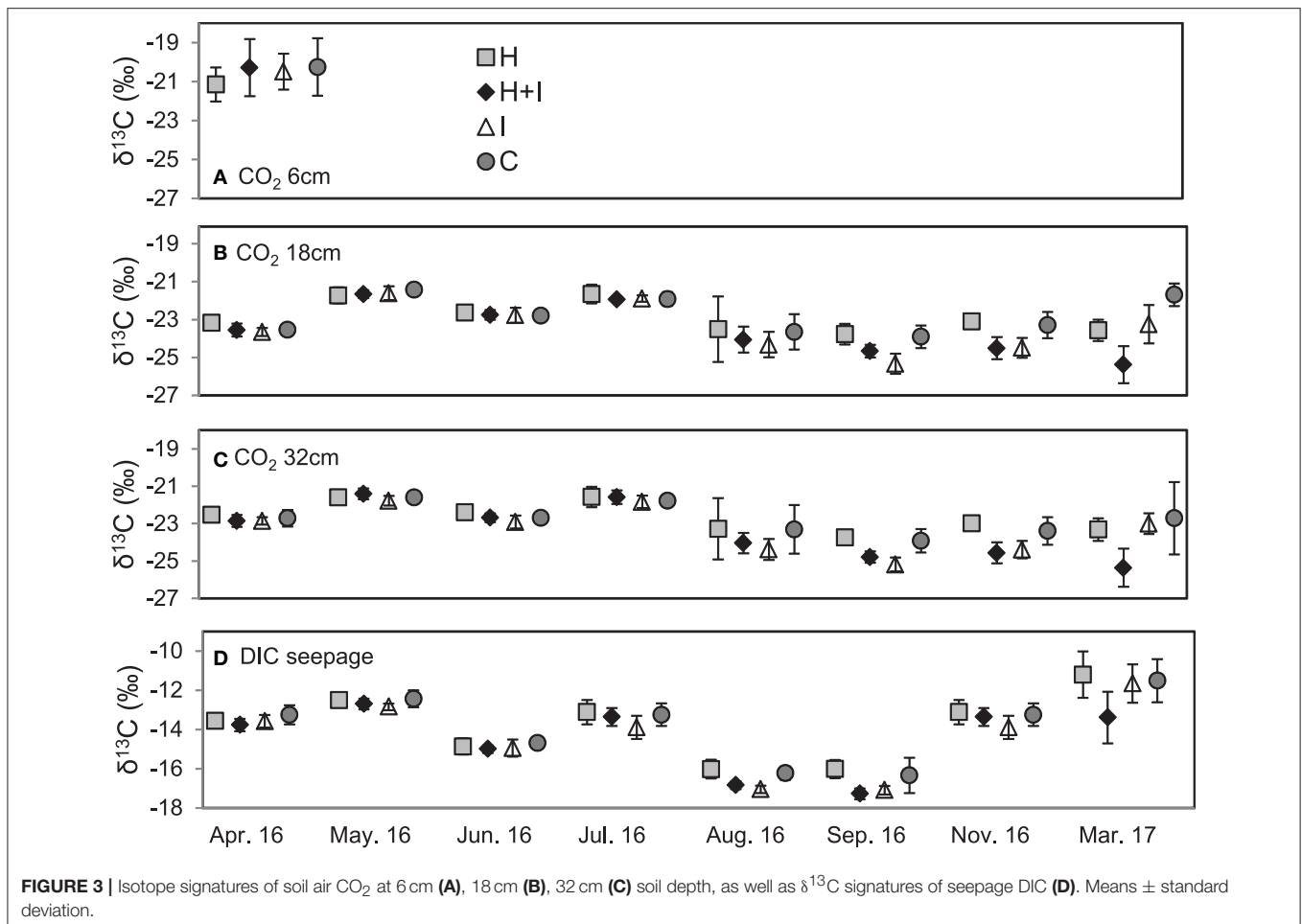
DOC Leaching

DOC leaching was four to five times lower than DIC leaching and differences between treatments were corresponding subtle in absolute amounts of carbon loss (Table 1). Similarly to DIC leaching, total annual DOC leaching losses were significantly ($p < 0.001$) higher in irrigated lysimeters (I and H+I). Furthermore, DOC leaching in H+I was significantly ($p = 0.01$) higher than in I (Table 1).

Soil Air CO_2 and Soil CO_2 Efflux

Soil air CO_2 concentrations ranged between 800 and 8,000 ppm in 6 cm soil depth and between 1,500 and 24,000 ppm in 18 cm soil depth. There was no further concentration increase from 18 to 32 cm soil depth and soil air CO_2 concentrations at all soil depths showed a typical temporal convergence with soil temperature (Figure 5). There was no significant treatment effect on soil air CO_2 concentrations at 6 cm soil depth. At 18 and 32 cm soil depth, irrigated lysimeters (I and H+I) showed significantly ($p < 0.001$) higher soil air CO_2 concentrations than C lysimeters, and H+I showed significantly higher concentrations when compared to H (Figure 5). Differences in soil air CO_2 concentrations were generally lower during the first treatment months and increased with treatment duration (treatment:date interaction $p < 0.05$). The seepage DIC concentrations were highly correlated to soil air CO_2 concentrations at 18 and 32 cm soil depth (Figure 6A).

Soil air $\delta^{13}\text{C}$ values ranged between -21.2 and -20.3% at 6 cm soil depth (single assessment in April 2016) and between -25.3 and -21.3% at 18 cm and -25.4 and -21.4% at 32 cm soil depth, respectively (Figure 3). The treatment effect on isotope ratios of soil air CO_2 at 18 and 32 cm depth was significant ($p < 0.001$), as was the treatment:date interaction ($p < 0.01$). Irrigated treatments (I and H+I) were on average about 0.5‰ depleted in ^{13}C , when compared to the non-irrigated treatments (C, H). The depletion became stronger during the latter treatment months (Figure 3). Linear regression analysis showed a significant ($p < 0.05$) relationship between seepage DIC $\delta^{13}\text{C}$ and soil air $\delta^{13}\text{C}$ values at 18 cm ($R^2 = 0.48$) and 32 cm ($R^2 = 0.54$) depth. Soil water $\delta^{13}\text{C}$ (HCO_3^- calculated after Equation 8) at 18 and 32 cm were strongly correlated with seepage DIC $\delta^{13}\text{C}$ as well (Figure 6B). The linear regression of the Keeling plot revealed an intercept of -24.0% for soil CO_2 at 6, 18, and



32 cm depth (Figure S3). Considering the isotopic enrichment of CO₂ of 4.4‰ by diffusion in the soil profile (Amundson et al., 1998), the corrected intercept was -28.4‰ . Thus, the Keeling plot approach resulted into an almost identical ^{13}C signature for soil CO₂ as the soil incubation (-28.5‰).

Soil CO₂ efflux immediately increased with soil warming and remained significantly ($p < 0.05$) and consistently accelerated throughout the whole two treatment years (Figure 2). Cumulative carbon efflux in the form of CO₂ efflux was significantly ($p < 0.01$) higher during the first treatment year

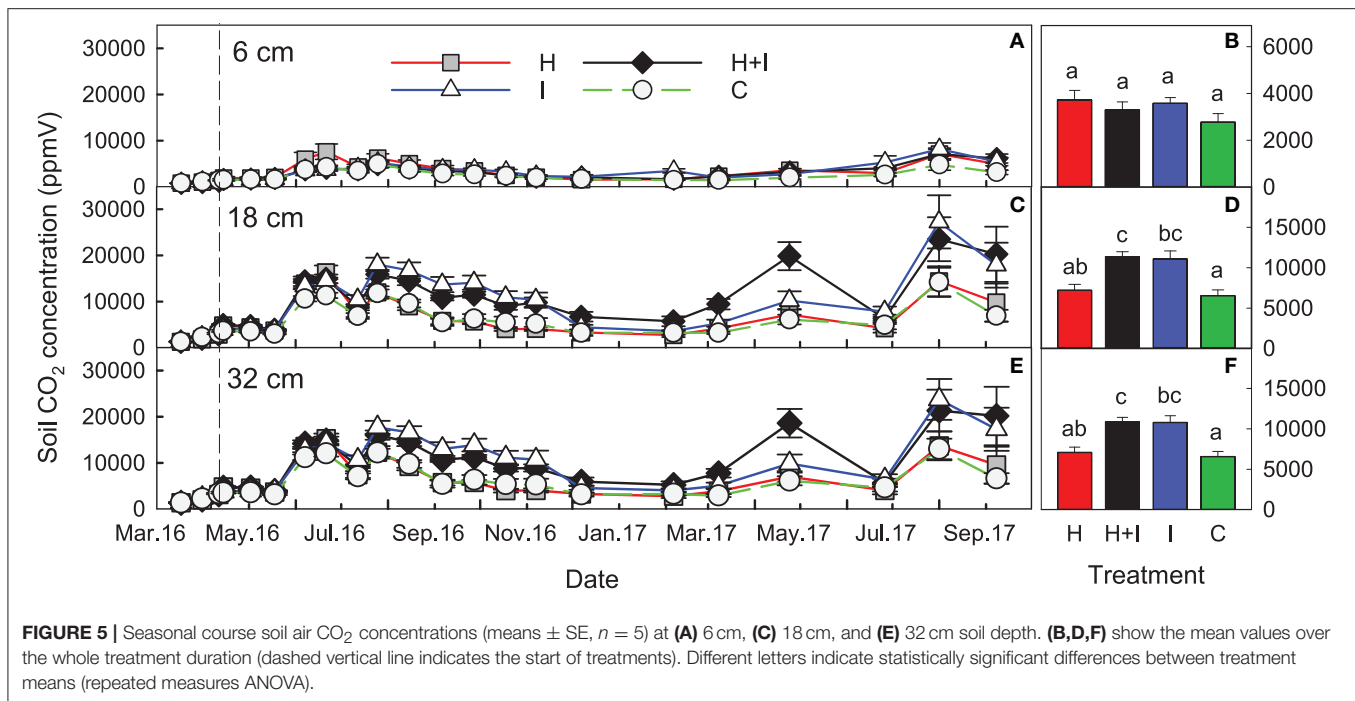


FIGURE 5 | Seasonal course soil air CO₂ concentrations (means \pm SE, $n = 5$) at (A) 6 cm, (C) 18 cm, and (E) 32 cm soil depth. (B,D,F) show the mean values over the whole treatment duration (dashed vertical line indicates the start of treatments). Different letters indicate statistically significant differences between treatment means (repeated measures ANOVA).

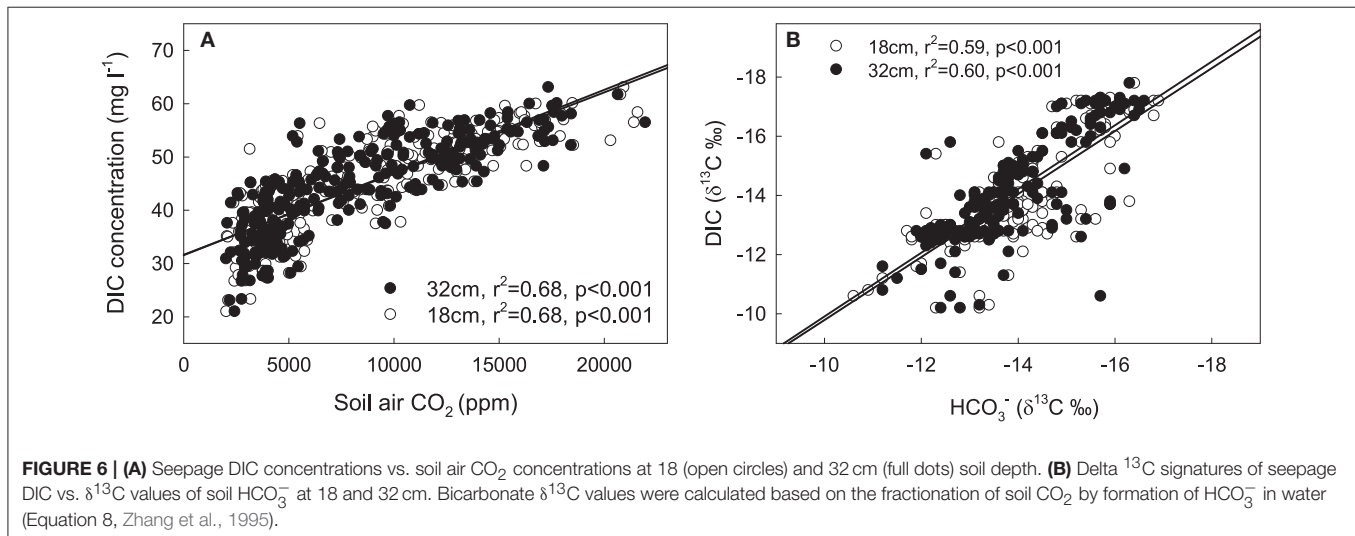


FIGURE 6 | (A) Seepage DIC concentrations vs. soil air CO₂ concentrations at 18 (open circles) and 32 cm (full dots) soil depth. (B) Delta ¹³C signatures of seepage DIC vs. ¹³C values of soil HCO₃⁻ at 18 and 32 cm. Bicarbonate ¹³C values were calculated based on the fractionation of soil CO₂ by formation of HCO₃⁻ in water (Equation 8, Zhang et al., 1995).

(Table 1) as well as over the whole experimental duration (Figure 2). Cumulative carbon loss via soil CO₂ efflux was 30–40% higher at warmed lysimeters, when compared to non-warmed lysimeters (Table 1; Figure 2). Irrigation had no significant effects on soil CO₂ efflux (Table 1; Figure 2).

DISCUSSION

We tried to elucidate the effects of potential climate changes on DIC leaching from a calcareous forest soil by artificially increasing soil temperature and precipitation in a model soil. The most striking observation in our study was that only increased

precipitation affected DIC leaching, whereas soil warming had no effects (Graphical Abstract). Accordingly, our original hypotheses were only partly confirmed. We initially hypothesized that soil warming would increase soil air CO₂ concentrations due to enhanced microbial respiration thereby increasing DIC concentrations in the soil solution (H1). This, however, was not observed. This was a surprise because soil was uniformly warmed down to the lower edge of the A-horizon (20 cm) and the soil CO₂ efflux was substantially enhanced by warming. There are basically two explanations. The more likely one is that soil warming simultaneously increased microbial respiration and soil diffusivity e.g., by lowering the water filled pore space. Soil moisture was indeed ~5 vol% lower during the summer

months at the warmed-only plots (**Figure 1**). Increased diffusion would allow for higher surface efflux at more or less unchanged soil air CO₂ concentrations. The other explanation is that most of the additional soil surface CO₂ efflux originated from the topsoil and litter layer. This explanation is less plausible since soil was warmed at two soil depths and organic carbon concentrations did not show a depth gradient in the homogenized A-horizons. It, however, cannot be excluded that a larger share of the total soil CO₂ efflux originated from the litter layer, and that this efflux was particularly affected by warming.

In comparison to warming, the irrigation treatments had pronounced effects on soil air CO₂ concentrations. Irrigation not only increased drainage (H2, H3), but also increased soil air CO₂ concentrations and thereby simultaneously increased the DIC concentrations in the soil solution and seepage. This shows that soil moisture strongly controls the gas diffusivity within the soil profile. The similar subsoil CO₂ concentrations in the I and H+I treatment or C and H treatment suggest elevated diffusion of CO₂ in the warmed lysimeters with partly drier top soils. Our hypotheses (H3) stating that the combination of warming and irrigation would result in highest DIC export, therefore, was refuted.

The isotopic mass balance approach using either the ¹³C signature of microbial respiration (−28.5‰) (Kindler et al., 2011) or the ¹³C signature of soil CO₂ at 18 cm depth suggest that most (60–100%) of DIC in seepage was of biotic origin and that only small fraction originated from dolomite weathering (**Figure 4**). According to the stoichiometry of carbonate dissolution (Equation 1), the biotic and abiotic fraction should approach a ratio of 1:1 at equilibrium conditions. An abiotic:biotic DIC ratio of 1:1 would require ¹³C signatures in DIC of about −5 to −8‰ using the isotopic mass balance approach. This indicates either that no chemical equilibrium was attained between seepage and dolomite weathering in our lysimeters and/or that the isotopic signature of DIC in seepage was driven by steady ¹³C exchange with gaseous soil CO₂. A ¹³C exchange between DIC and soil CO₂ seems very likely in our lysimeters, as the mean difference in the ¹³C signature of 9‰ between DIC and CO₂ at 32 cm depth matches the isotopic fractionation in the CO₂/HCO₃[−] system (Clark, 2015; **Figure 6**; **Figure S3**). Permanent production of soil CO₂ by microbial respiration strengthens the CO₂ imprint on the isotopic signature of DIC. This dominance becomes very clear when soil CO₂ at 18 cm depth was used for the mass balance approach (average 100% biotic DIC, **Figure 4**). The approach by Kindler et al. (2011) (average 76% biotic DIC) does not consider the isotopic fractionation of 4.4‰ for diffusion of CO₂ in the soil profile (Amundson et al., 1998). Therefore, under the open, or almost open system conditions, prevailing in our lysimeters, δ¹³C values of DIC, and the corresponding mass balance approach (Equation 6), seem rather unfeasible for an accurate partitioning between biotic and abiotic DIC sources. In agreement with our results, Eshel and Singer (2016) showed that dissolving calcite did not affect the ¹³C signature of DIC in a controlled laboratory setup simulating an open system.

An overestimation of the biotic DIC fraction or underestimation of the abiotic DIC fraction could further

arise from dolomite weathering by other acids than carbonic acid. Weathering of dolomite by none-carbonic acids alters the isotopic mass balance approach by enriching the ¹³C signature of DIC toward the ¹³C signature of dolomite. Especially the production of protons by nitrification associated with leaching of nitrate is critical for the isotopic mass balance approach (Jin et al., 2009; Li and Ji, 2016). We found relatively high nitrate concentrations of 80 mg l^{−1} in seepage after subtraction of nitrate input by rainwater (unpublished data). Nitrate leaching was very high in our lysimeters due to missing uptake by plants. When 1 mol of nitrate corresponds to 1 mol bicarbonate in seepage, nitrification would account for roughly 40% of total DIC in seepage. Although nitrate concentration is smaller in seepage at the soil collection site (Feichtinger et al., 2002), nitrification could also be an important player for DIC leaching at the field site in the Northern Limestone Alps. The relative and absolute proportion of biotic DIC could vary with season as several processes are involved in the DIC production. Even though our experiment provides a first estimation, it suggests, that DIC partitioning is complex and constrained by several factors. Although it remains challenging to estimate the exact absolute biotic contribution to DIC, we here could show that the different treatments did not affect the contribution of biotic carbon (**Figure 4**). The isotopic composition of DIC changed seasonally, but all treatments showed the same trend, indicating that warming and irrigation, or a combination of both, had no influence on the share of biotic and abiotic carbon in DIC.

DIC leaching from the studied carbonate forest soil amounted up to 5% of the total annual lysimeter-soil carbon loss. Annual DIC leaching rates of between 20 (control) and 40 (irrigated) g C m^{−2} y^{−1} were above the typical leaching rates of acidic forest soils (average 11 g C m^{−2}) but similar to that of higher pH grassland and arable soils (Kindler et al., 2011). DIC leaching from another, similar, calcareous forest soil was estimated at around 10 g C m^{−2} y^{−1} by Bader et al. (2013), but since only the top 15 cm of the 30 cm soil profile were accounted for, the total leaching rates may lay close to our observations. The irrigation treatments suggest that precipitation strongly controls DIC leaching from calcareous soils and that DIC leaching is a particularly important component of the soil C budget in regions with high precipitation.

We are aware that the applied lysimeter approach cannot substitute field measurements and field experiments because of missing trees, exclusion of roots, mycorrhiza, soil disturbance etc. While we could show that the response of DIC flux to soil warming and irrigation, as well as the combination of both, can be disentangled by our experimental approach, it does not fully resemble natural field conditions. At the field site, roots considerably contribute to soil respiration and affect the soil CO₂ concentration in the rhizosphere (Schindlbacher et al., 2009; Díaz-Pinés et al., 2010). Soil CO₂ efflux from the lysimeters (only heterotrophic) was in a similar range than the total soil CO₂ efflux (heterotrophic + autotrophic) in the field, though it was expected to be ~50% lower due to lacking rhizosphere contribution. The higher soil CO₂ fluxes from the lysimeters, however, can be explained by the overall higher temperatures at the lysimeter site. Especially summer soil temperatures, during

which CO₂ fluxes peaked, were more than 5°C higher at the lysimeter site than at the Achenkirch site. The high CO₂ fluxes from the lysimeters might have also been partly caused by the release of labile carbon during soil disturbance during coarse-sieving and soil re-packing. It is, however, rather unlikely that this played a big role, as field soil is highly bioturbated and has a naturally lightly and crumbly structure. Furthermore, release of labile carbon should have caused rather ephemeral increases in soil CO₂ efflux, which were, however, not visible in our 2 year soil CO₂ record (**Figure 2**). The response of the soil CO₂ efflux to the 4°C warming treatment was very similar as during the initial years of the field warming experiment (Schindlbacher et al., 2009) and, as hypothesized, precipitation manipulation had no significant effects on soil CO₂ efflux because SOM decomposition was not water limited during most of the 2 years.

As hypothesized, DOC leaching was low and contributed <1% to the annual total soil carbon loss. Similar DOC loss rates were reported for a Rendzina and a Cambisol where DOC leaching dropped with increasing thickness of the mineral soil (Kammer et al., 2012). A large part of DOC originated from the thin litter layer that mainly consisted of beech leaves from the preceding litterfall. DOC leaching from root litter can be largely excluded in our lysimeter experiment. Hence, DOC leaching could make a slightly greater contribution to the soil C budget in undisturbed soils with an intact root system.

Our results and results of other studies (Hagedorn et al., 2010; Fröberg et al., 2013) indicate that soil warming does not increase DOC leaching from forest soils. Elevated soil microbial activity in the warmed plots had obviously no effect on the leachable DOC pool. Precipitation or the resulting soil water drainage, however, strongly controlled DOC leaching. The increase in precipitation by 50% entailed a similar increase in DOC leaching suggesting a certain linearity between DOC leaching and soil water flux. This finding is supported by other irrigation experiments (Fröberg et al., 2013) although the irrigation effect could diminish in the long run (Kalbitz et al., 2007). On a regional scale, the effect of precipitation on subsoil DOC leaching was about twice as strong as in this lysimeter experiment (Borken et al., 2011).

CONCLUSIONS

We could show that particularly rising precipitation could increase DIC leaching from calcareous soils, whereas soil warming has likely little effect. A future increase in annual precipitation is a possible scenario for the Alps (Torma et al., 2015) and would lead to increased drainage losses of soil carbon.

REFERENCES

- Amiotte-Suchet, P., Aubert, D., Probst, J.-L., Gauthier-Lafaye, F. O., Probst, A., Andreux, F., et al. (1999). $\delta^{13}\text{C}$ pattern of dissolved inorganic carbon in a small granitic catchment: the Strengbach case study (Vosges mountains, France). *Chem. Geol.* 159, 129–145. doi: 10.1016/S0009-2541(99)00037-6
- Amundson, R., Stren, L., Baisden, T., and Wang, Y. (1998). The isotopic composition of soil and soil-respired CO₂. *Geoderma* 82, 83–114.
- Bader, M. K. F., Leuzinger, S., Keel, S. G., Siegwolf, R. T. W., Hagedorn, F., Schleppe, P., et al. (2013). Central European hardwood trees in a high-CO₂ future: synthesis of an 8-year forest canopy CO₂ enrichment project. *J. Ecol.* 101, 1509–1519. doi: 10.1111/1365-2745.12149
- Borken, W., Ahrens, B., Schulz, C., and Zimmermann, L. (2011). Site-to-site variability and temporal trends of DOC concentrations and fluxes in temperate forest soils. *Glob. Change Biol.* 17, 2428–2443. doi: 10.1111/j.1365-2486.2011.02390.x
- Considering that a part of DIC is degassing from streams into the atmosphere (Oquist et al., 2009; Shin et al., 2011), increasing precipitation and DIC leaching triggered by climate change would have a positive feedback to the CO₂ concentration of the atmosphere. This effect is, however, small when compared to the potential warming induced carbon losses through increased SOM decomposition and increased soil CO₂ efflux. Our results also suggest that partitioning of DIC fluxes into biotic and abiotic (carbonate weathering) compounds requires the consideration of other acids than carbonic acids that contribute to the weathering of carbonate and production of bicarbonate.

DATA AVAILABILITY

Datasets are available on request. The raw data supporting the conclusions of this manuscript will be made available by the authors, without undue reservation, to any qualified researcher.

AUTHOR CONTRIBUTIONS

KB performed DIC, DOC, and CO₂ sampling and measurements and contributed to data analysis. SH constructed the soil warming system, the temperature, and soil moisture monitoring system. AS analyzed the data and wrote the first draft of the manuscript. KB and WB contributed to the manuscript writing. WB designed the experimental setup.

FUNDING

We acknowledge the financial support by the German Research Foundation (DFG Project 397643203).

ACKNOWLEDGMENTS

We like to thank Uwe Hell, Gerhard Müller, and Oliver Archner for setup of the lysimeter experiment and data monitoring and Karin Söllner for laboratory help. ¹³C analyses were performed by the Laboratory of Isotope Biogeochemistry of the BayCEER, University of Bayreuth and the Centre for Stable Isotope Research and Analysis at the University of Göttingen.

SUPPLEMENTARY MATERIAL

The Supplementary Material for this article can be found online at: <https://www.frontiersin.org/articles/10.3389/ffgc.2019.00040/full#supplementary-material>

- Borken, W., and Matzner, E. (2009). Reappraisal of drying and wetting effects on C and N mineralization and fluxes in soils. *Glob. Change Biol.* 15, 808–824. doi: 10.1111/j.1365-2486.2008.01681.x
- Camino-Serrano, M., Gielen, B., Luysaert, S., Ciais, P., Vicca, S., Guenet, B., et al. (2014). Linking variability in soil solution dissolved organic carbon to climate, soil type, and vegetation type. *Glob. Biogeochem. Cycles* 28, 497–509. doi: 10.1002/2013GB004726
- Christophel, D., Höllerl, S., Prietzel, J., and Steffens, M. (2015). Long-term development of soil organic carbon and nitrogen stocks after shelterwood- and clear-cutting in a mountain forest in the Bavarian Limestone Alps. *Eur. J. For. Res.* 134, 623–640. doi: 10.1007/s10342-015-0877-z
- Clark, I. (2015). *Groundwater Geochemistry and Isotopes*. Boca Raton, FL: CRC press.
- Davidson, E. A., Savage, K. E., Trumbore, S. E., and Borken, W. (2006). Vertical partitioning of CO₂ production within a temperate forest soil. *Glob. Change Biol.* 12, 944–956. doi: 10.1111/j.1365-2486.2006.01142.x
- Díaz-Pinés, E., Schindlbacher, A., Pfeffer, M., Jandl, R., Zechmeister-Boltenstern, S., and Rubio, A. (2010). Root trenching - A useful tool to estimate autotrophic soil respiration? Case study in an Austrian mountain forest. *Eur. J. Forest Res.* 129, 101–109. doi: 10.1007/s10342-008-0250-6
- Eshel, G., and Singer, M. J. (2016). Inorganic carbon transformations between phases and its impact on its isotopic signature under open conditions. *Geoderma* 273, 20–24. doi: 10.1016/j.geoderma.2016.03.014
- Fang, C., and Moncrieff, J. (2001). The dependence of soil CO₂ efflux on temperature. *Soil Biol. Biochem.* 33, 155–165. doi: 10.1016/S0038-0717(00)00125-5
- FAO (1998). *World Reference Base for Soil Resources*. Rome: Food and Agriculture Organization of the United Nations.
- Feichtinger, F., Smidt, S., and Klaghofer, E. (2002). Water and nitrate fluxes at a forest site in the North Tyrolean Limestone Alps. *Environ. Sci. Pollut. Res.* 9, 31–36. doi: 10.1007/BF02987475
- Frei, C., and Schär, C. (1998). A precipitation climatology of the Alps from high-resolution rain-gauge observations. *Int. J. Climatol.* 18, 873–900.
- Fröberg, M., Grip, H., Tipping, E., Svensson, M., Strömberg, M., and Kleja, D. B. (2013). Long-term effects of experimental fertilization and soil warming on dissolved organic matter leaching from a spruce forest in Northern Sweden. *Geoderma* 200, 172–179. doi: 10.1016/j.geoderma.2013.02.002
- Hagedorn, F., Martin, M., Rixen, C., Rusch, S., Bebi, P., Zürcher, A., et al. (2010). Short-term responses of ecosystem carbon fluxes to experimental soil warming at the Swiss alpine treeline. *Biogeochemistry* 97, 7–19. doi: 10.1007/s10533-009-9297-9
- IPCC (2013). “Climate Change 2013: The physical science basis.” in *Contribution of Working Group I to the Fifth Assessment Report of the Intergovernmental Panel on Climate Change*, eds T. F. Stocker, D. Qin, G. K. Plattner, M. Tignor, S. K. Allen, J. Boschung, A. Nauels, Y. Xia, B. Bex, and B.M. Midgley (Cambridge; New York, NY: Cambridge University Press), 1535.
- Jin, L., Ogrinc, N., Hamilton, S. K., Szramek, K., Kanduc, T., and Walter, L. M. (2009). Inorganic carbon isotope systematics in soil profiles undergoing silicate and carbonate weathering (Southern Michigan, USA). *Chem. Geol.* 264, 139–153. doi: 10.1016/j.chemgeo.2009.03.002
- Kalbitz, K., Meyer, A., Yang, R., and Gerstberger, P. (2007). Response of dissolved organic matter in the forest floor to long-term manipulation of litter and throughfall inputs. *Biogeochemistry* 86, 301–318. doi: 10.1007/s10533-007-9161-8
- Kammer, A., Schmidt, M. W. I., and Hagedorn, F. (2012). Decomposition pathways of 13C-depleted leaf litter in forest soils of the Swiss Jura. *Biogeochemistry* 108, 395–411. doi: 10.1007/s10533-011-9607-x
- Karberg, N. J., Pregitzer, K. S., King, J. S., Friend, A. L., and Wood, J. R. (2005). Soil carbon dioxide partial pressure and dissolved inorganic carbonate chemistry under elevated carbon dioxide and ozone. *Oecologia* 142, 296–306. doi: 10.1007/s00442-004-1665-5
- Keeling, C. D. (1961). The concentration and isotopic abundances of carbon dioxide in rural and marine air. *Geochim. Cosmochim. Acta* 24, 277–298. doi: 10.1016/0016-7037(61)90023-0
- Kindler, R., Siemens, J. A. N., Kaiser, K., Walmsley, D. C., Bernhofer, C., Buchmann, N., et al. (2011). Dissolved carbon leaching from soil is a crucial component of the net ecosystem carbon balance. *Glob. Change Biol.* 17, 1167–1185. doi: 10.1111/j.1365-2486.2010.02282.x
- Kloss, S., Sass, O., Geitner, C., and Prietzel, J. (2012). Soil properties and charcoal dynamics of burnt soils in the Tyrolean Limestone alps. *CATENA* 99, 75–82. doi: 10.1016/j.catena.2012.07.011
- Li, C., and Ji, H. (2016). Chemical weathering and the role of sulfuric and nitric acids in carbonate weathering: Isotopes (13C, 15N, 34S, and 18O) and chemical constraints. *J. Geophys. Res.* 121, 1288–1305. doi: 10.1002/2015JG003121
- Ogrinc, N., Kanduč, T. A., Krajnc, B., Vilhar, U. A., Simončič, P., and Jin, L. (2016). Inorganic and organic carbon dynamics in forested soils developed on contrasting geology in Slovenia—a stable isotope approach. *J. Soils Sediments* 16, 382–395. doi: 10.1007/s11368-015-1255-7
- Oquist, M. G., Wallin, M., Seibert, J., Bishop, K., and Laudon, H. (2009). Dissolved inorganic carbon export across the soil/stream interface and its fate in a boreal headwater stream. *Environ. Sci. Technol.* 43, 7364–7369. doi: 10.1021/es900416h
- Orchard, V. A., and Cook, F. J. (1983). Relationship between soil respiration and soil moisture. *Soil Biol. Biochem.* 15, 447–453. doi: 10.1016/0038-0717(83)90010-X
- Prietzel, J., and Christophel, D. (2014). Organic carbon stocks in forest soils of the German Alps. *Geoderma* 221, 28–39. doi: 10.1016/j.geoderma.2014.01.021
- Prietzel, J., Zimmermann, L., Schubert, A., and Christophel, D. (2016). Organic matter losses in German Alps forest soils since the 1970s most likely caused by warming. *Nat. Geosci.* 9, 543–548. doi: 10.1038/ngeo2732
- Sander, R. (2015). Compilation of Henry’s law constants (version 4.0) for water as solvent. *Atmosphere. Chem. Phys.* 15, 4399–4981. doi: 10.5194/acp-15-4399-2015
- Savage, K. E., and Davidson, E. A. (2003). A comparison of manual and automated systems for soil CO₂ flux measurements: trade-offs between spatial and temporal resolution. *J. Exp. Bot.* 54, 891–899. doi: 10.1093/jxb/erg121
- Schindlbacher, A., Borken, W., Djukic, I., Brandstätter, C., Spötl, C., and Wanek, W. (2015a). Contribution of carbonate weathering to the CO₂ efflux from temperate forest soils. *Biogeochemistry* 124, 273–290. doi: 10.1007/s10533-015-0097-0
- Schindlbacher, A., De Gonzalo, C., Díaz-Pinés, E., Gorriá, P., Matthews, B., Inclán, R., et al. (2010). Temperature sensitivity of forest soil organic matter decomposition along two elevation gradients. *J. Geophys. Res.* 115:G03018. doi: 10.1029/2009JG001191
- Schindlbacher, A., Schneckler, J., Takriti, M., Borken, W., and Wanek, W. (2015b). Microbial physiology and soil CO₂ efflux after 9 years of soil warming in a temperate forest – no indications for thermal adaptations. *Glob. Change Biol.* 21, 4265–4277. doi: 10.1111/gcb.12996
- Schindlbacher, A., Wunderlich, S., Borken, W., Kitzler, B., Zechmeister-Boltenstern, S., and Jandl, R. (2012). Soil respiration under climate change: prolonged summer drought offsets soil warming effects. *Glob. Change Biol.* 18, 2270–2279. doi: 10.1111/j.1365-2486.2012.02696.x
- Schindlbacher, A., Zechmeister-Boltenstern, S., and Jandl, R. (2009). Carbon losses due to soil warming: do autotrophic and heterotrophic soil respiration respond equally? *Glob. Change Biol.* 15, 901–913. doi: 10.1111/j.1365-2486.2008.01757.x
- Shin, W. J., Chung, G. S., Lee, D., and Lee, K. S. (2011). Dissolved inorganic carbon export from carbonate and silicate catchments estimated from carbonate chemistry and δ¹³C DIC. *Hydrol. Earth Syst. Sci.* 15, 2551–2560. doi: 10.5194/hess-15-2551-2011
- Siemens, J., Pacholski, A., Heiduk, K., Giesemann, A., Schulte, U., Dechow, R., et al. (2012). Elevated air carbon dioxide concentrations increase dissolved carbon leaching from a cropland soil. *Biogeochemistry* 108, 135–148. doi: 10.1007/s10533-011-9584-0
- Smiatek, G., Kunstmann, H., and Senatore, A. (2016). EURO-CORDEX regional climate model analysis for the greater alpine region: performance and expected future change. *J. Geophys. Res.* 121, 7710–7728. doi: 10.1002/2015JD024727
- Szramek, K., McIntosh, J. C., Williams, E. L., Kanduc, T., Ogrinc, N., and Walter, L. M. (2007). Relative weathering intensity of calcite versus dolomite in carbonate-bearing temperate zone watersheds: carbonate geochemistry and fluxes from catchments within the St. Lawrence and Danube river

- basins. *Geochem. Geophys. Geosyst.* 8:Q04002. doi: 10.1029/2006GC001337
- Torma, C., Giorgi, F., and Coppola, E. (2015). Added value of regional climate modeling over areas characterized by complex terrain-Precipitation over the Alps. *J. Geophys. Res.* 120, 3957–3972. doi: 10.1002/2014JD022781
- Vogel, J. C., Grootes, P. M., and Mook, W. G. (1970). Isotopic fractionation between gaseous and dissolved carbon dioxide. *Zeitschrift für Physik Hadrons Nuclei* 230, 225–238. doi: 10.1108/eb034609
- Zhang, J., Quay, P. D., and Wilbur, D. O. (1995). Carbon isotope fractionation during gas-water exchange and dissolution of CO₂. *Geochim. Cosmochim. Acta* 59, 107–114.

Conflict of Interest Statement: The authors declare that the research was conducted in the absence of any commercial or financial relationships that could be construed as a potential conflict of interest.

Copyright © 2019 Schindlbacher, Beck, Holzheu and Borken. This is an open-access article distributed under the terms of the Creative Commons Attribution License (CC BY). The use, distribution or reproduction in other forums is permitted, provided the original author(s) and the copyright owner(s) are credited and that the original publication in this journal is cited, in accordance with accepted academic practice. No use, distribution or reproduction is permitted which does not comply with these terms.